J Therm Anal Calorim (2010) 102:941–951
DOI 10.1007/s10973-010-0841-6

Study of the hydration of Portland cement blended with blast-furnace slag by calorimetry and thermogravimetry

E. Gruyaert · N. Robeyst · N. De Belie

Received: 4 February 2010 / Accepted: 22 April 2010 / Published online: 11 May 2010

Abstract The hydration of ordinary Portland cement (OPC) blended with blast-furnace slag (BFS) is a complex process since both materials have their own reactions which are, however, influenced by each other. Moreover, the effect of the slag on the hydration process is still not entirely known and little research concerning the separation of both reactions can be found in the literature. Therefore, this article presents an investigation of the hydration process of mixes in which 0–85% of the OPC is replaced by BFS. At early ages, isothermal, semi-adiabatic and adiabatic calorimetric measurements were performed to determine the heat of hydration. At later ages, thermogravimetric (TG) analyses are more suitable to follow up the hydration by assessment of the bound water content w_b. In addition, the microstructure development was visualized by backscattered electron (BSE) microscopy. Isothermal calorimetric test results show an enhancement of the cement hydration and an additional hydration peak in the presence of BFS, whilst (semi-)adiabatic calorimetric measurements clearly indicate a decreasing temperature rise with increasing BFS content. Based on the cumulative heat production curves, the OPC and BFS reactions were separated to determine the reaction degree $Q(t)/Q_\infty$ (Q = cumulative heat production) of the cement, slag and total binder. Moreover, thermogravimetry also allowed to calculate the reaction degree by $w_b(t)/w_{b\infty}$. The reaction degrees $w_b(t)/w_{b\infty}$, $Q(t)/Q_\infty$ and the hydration degrees determined by BSE-image analysis showed quite good correspondence.

Keywords Blast-furnace slag · Hydration · Calorimetry · Bound water

E. Gruyaert · N. Robeyst · N. De Belie (✉)
Magnel Laboratory for Concrete Research, Ghent University, Technologiepark Zwijnaarde 904, 9052 Ghent, Belgium
e-mail: Nele.Debelie@UGent.be

Introduction

The hydration of the cement minerals C_3S ($3CaO{\cdot}SiO_2$), C_2S ($2CaO{\cdot}SiO_2$), C_3A ($3CaO{\cdot}Al_2O_3$) and C_4AF ($4CaO{\cdot}Al_2O_3{\cdot}Fe_2O_3$) is an exothermal chemical process. At early ages, the generated heat can be monitored by isothermal (conduction) calorimetry and five stages can be distinguished, as mentioned by several researchers [1, 2]: (i) the initial period; (ii) the induction period; (iii) the acceleration period; (iv) the deceleration period and (v) the period of slow continued reaction.

The possibility to detect the first hydration peak, associated with the wetting of cement and the hydration of free lime, C_3A and hemi-hydrate ($CaSO_4{\cdot}0.5H_2O$), depends on the calorimeter design [1, 3]. Different methods which allow mixing inside the calorimeter and consequently favour the detection of the first hydration peak, can be found in the literature [4, 5]. Contrarily, the second peak, due to the hydration of C_3S can always be registered completely. Additionally, a third peak sometimes appears due to the hydration of C_3A (the reaction of ettringite to monosulphate [6]). According to Bensted [7] only a C_3A amount of more than 12% results in a visible third peak at 20 °C. However, in presence of fly ash, Baert [8] already recorded this peak for cement containing merely 7.5% C_3A.

When ordinary Portland cement (OPC) is partially replaced by blast-furnace slag (BFS), the reaction of BFS is activated by the release of hydroxyl ions. Although NaOH and KOH are the major components after about 1 day of hydration, rather than $Ca(OH)_2$ (CH), the presence of solid CH ensures that the supply of OH^- ions is maintained [9, 10]. According to some researchers [11, 12], this activation is effective when the pH of the aqueous phase is higher than 11.5 due to cement hydration or alkali-activation, whilst others claim a value of 12

[3]. From then onwards, the reaction of BFS with CH takes place and continues due to the progressive release of alkalis by BFS and the formation of CH by OPC [13]. Moreover, the curves of the heat production rate in function of time show an extra peak caused by the hydration of BFS, as generally accepted by, e.g. [14–16]. Depending on the slag characteristics and the hydration temperature, this additional peak is completely separated from the OPC hydration peaks or appears as a 'shoulder' [15, 16]. Concerning the influence of BFS on the OPC hydration, different research results disagree. According to [15], the OPC hydration peak appears at the same moment independent from the presence of slag. On the other hand, the research performed by Singh et al. [17] on Portland cement blended with bag house dust and granulated BFS indicates that GBFS retards the hydration of the silicate phase and delays the conversion of ettringite to monosulphate. Conversely, [3, 18] demonstrated that BFS accelerates the OPC hydration. Different mechanisms to explain the effect of BFS on the OPC hydration, which can be found in the literature, are summarized below:

(1) Escalante-Garcia and Sharp [18] attribute the enhanced hydration of the four anhydrous phases to the dilution effect, favouring the dissolution of cement grains and consequently enhancing the hydration of the interstitial phases. However, isothermal calorimetric tests performed by Baert [8] on cement pastes show no acceleration of the second hydration peak with increasing water-to-cement ratios ($0.3 \rightarrow 0.4 \rightarrow 0.5$), although the second peak broadens and the hydration degree at 7 days increases.
(2) Since CH, liberated during the alite hydration, is believed to be consumed during the BFS reaction, the equilibrium is shifted towards a more advanced OPC hydration [18].
(3) Uchikawa (cited by [18]) claims that the hydration of interstitial phases is accelerated due to the fixation of Ca^{2+} and SO_4^{2-} by the slag.
(4) According to Stark et al. [19], the reaction of the alite/clinker with water can be accelerated by adding mineral admixtures with a high specific surface area and a high chemical affinity towards calcium silicate hydrate (C–S–H) phases. Since C–S–H is first formed on the fine materials, no layer is formed covering the C_3S surface. In this way, dissolution of alite can proceed unrestrictedly, leading to a higher degree of hydration of this clinker mineral. For BFS, which possesses a low chemical affinity, this accelerating effect can only be attained when the specific surface area is very high.
(5) D'Aloia and Chanvillard [20] also found that the molar ratio $n\mathrm{SO_3}/n\mathrm{C_3A}$ determines the importance of the conversion reaction of ettringite to monosulphate. When this ratio increases, the conversion becomes less pronounced and does not occur anymore at a value of 3. In this case, only ettringite remains and the corresponding hydration peak is higher and less broad. Since the replacement of cement by BFS changes the molar ratio of SO_3 to C_3A, the above-mentioned reaction mechanisms and consequently the evolution of the heat production rate in function of time can change.

Isothermal calorimetry also seems to be a good tool to determine the reaction degree. In contrast to the hydration degree, defined as the cement fraction that has reacted, the reaction degree can be more easily determined and is calculated as the heat released at a certain moment $Q(t)$ relative to the maximum heat release Q_{max} [14]. Pane and Hansen [21] also affirmed the suitability of the method for blended cements. Moreover, they demonstrate the similar trend between $Q(t)/Q(\infty)$ and $w_b(t)/w_b(\infty)$, indicating that the chemically bound water content (w_b), determined by thermogravimetric (TG) analyses, also measures the degree of reaction. According to Hewlett [10], the non-evaporable water content is only an 'indicator' of the progress of the OPC hydration and is not useful in determining the hydration degree of cements blended with pozzolanic materials because of the change in amount and chemical composition of the hydrates. Nonetheless, results of OPC and blended cements can be compared to detect the differences in hydration process between both.

In this research, isothermal calorimetric measurements and TG analyses were performed on pastes in which a (large) part of the cement was replaced by BFS. Besides the isothermal calorimetric measurements, semi-adiabatic and adiabatic calorimetric measurements were executed on mortar or concrete. In comparison to the calorimetric tests performed by De Schutter [14, 22] on blended cements, the BFS was here added as a separate component to the concrete mix and the slag-to-binder ratios varied between 0 and 85%. Moreover, backscattered electron (BSE) images were taken in a scanning electron microscope to visualize the hydration reactions and to determine the amount of remaining unhydrated cement and slag at a certain moment. Consequently the hydration degree of both binders could be calculated and compared with the reaction degree determined by calorimetry ($Q(t)/Q_\infty$) and TG ($w_b(t)/w_{b\infty}$).

Materials and methods

Materials

Ordinary Portland cement CEM I 52.5 N (EN 197-1) was used for all paste, mortar and concrete mixes. Besides the reference mixes, containing only OPC as binder, mixes in

Table 1 Chemical composition/% and Blaine fineness/m^2 kg^{-1} of the Portland cement and BFS

	CaO	SiO_2	Al_2O_3	Fe_2O_3	MgO	SO_3	CO_2	Blaine
OPC-CAL	62.2	18.8	5.4	3.8	0.9	3.1	0.7	390
OPC-CAL/extra	63.4	18.9	5.7	4.3	0.9	3.3	0.5	353
OPC-TG/a	63.1	18.7	4.9	4.0	1.0	3.1	0.7	359
OPC-TG/b	62.2	18.8	5.4	3.8	0.9	3.1	0.7	390
BFS-CAL	40.4	34.4	11.4	0.5	7.6	1.7	0.3	400
BFS-CAL/extra	41.2	36.4	9.8	0.3	7.4	1.6	0.9	339
BFS-TG/a	42.6	33.9	8.9	0.7	7.4	1.6	0.4	397
BFS-TG/b	40.4	34.4	11.4	0.5	7.6	1.7	0.3	400

CAL material for calorimetry, *CAL/extra* material used for additional experiments to investigate the effect of the dilution effect, *TG* material for thermogravimetry, *TG/a* measurements at an age <2 days, *TG/b* measurements at an age >2 days

which 15–85% of the cement was replaced by BFS were made. As the calorimetric and thermogravimetric measurements were performed on mixes containing OPC and BFS from different batches, Table 1 summarizes the chemical composition and Blaine fineness of the OPC and BFS used in this research. Only a slight difference can be noticed between the batches.

Isothermal calorimetric measurements

In this study, the hydration heat of OPC and BFS was determined with an isothermal heat conduction calorimeter (TAM AIR—TA instruments). Each channel of this calorimeter is constructed in twin configuration with one side for the test sample and the other side for an inert reference (quartz sand). Beneath each channel, heat flow sensors are installed to measure the heat production rate q (mW/g). The twin principle allows the heat flow from the active sample to be compared with the reference. This comparison enhances the stability and limits the noise within the system.

Isothermal calorimetric measurements were performed at 283 K (10 °C), 293 K (20 °C) and 308 K (35 °C). Each sample ampoule contained 14 g paste consisting of OPC, BFS and water. The water-to-binder ratio (w/b) amounted to 0.5 and the slag-to-binder ratios (s/b) were 0, 0.30, 0.50 and 0.85. Before mixing, the components were kept at a temperature close to the measurement temperature to avoid significant differences between the paste and the isothermal environment. Subsequently, the components were manually mixed together. Since mixing occurred outside the calorimeter, the first hydration peak could not be registered entirely. This peak only amounts to a few per cent of the total heat liberated [22] and will therefore not be considered in the further analysis.

Semi-adiabatic calorimetric measurements

During semi-adiabatic measurements (Langavant calorimeter) the temperature rise of a hydrating mortar or concrete sample is measured. Considering the thermal capacity and heat losses of the test setup, the cumulative heat production Q (J/g) can then be calculated according to EN 196-9. Moreover, the heat production rate q was calculated as the derivative of Q and presented in function of time.

In this study, semi-adiabatic calorimetric measurements were performed on standard mortars (EN 196-1) and concrete mixtures. A standard mortar mixture consists of 1350 g sand, 225 g water and 450 g cement. In this research, the cement was partially replaced by BFS and the s/b ratios were 0, 0.15, 0.30, 0.50, 0.70 and 0.85. The concrete mixes had a w/b of 0.5 and s/b of 0, 0.30, 0.50, 0.70 and 0.85. The composition for 1 m^3 reference (OPC) concrete was: 350 kg OPC, 175 kg water, 791 kg sand 0/4, 425 kg gravel 2/8 and 618 kg gravel 8/16.

In contrast to the measurements on concrete samples, lasting only 48 h, the measurements on mortar samples were performed during 14 days. Although the hydration proceeds for a longer time, most of the hydration heat is liberated during the first days after mixing. Therefore, the heat production after 14 days is here considered to be the total heat production (Q_{total}).

Adiabatic calorimetric measurements

Contrary to semi-adiabatic measurements, during which a limited heat exchange with the environment is allowed, the heat exchange is completely avoided under adiabatic conditions by keeping the environment at the same temperature as the hydrating concrete sample. A detailed description of the setup can be found in [22]. Since it took some time to instal the concrete sample in the calorimeter, measurements were started 40 min after water addition.

Adiabatic calorimetric measurements were performed on concrete mixes with a w/b ratio of 0.5 and s/b ratios of 0, 0.15, 0.30, 0.50, 0.70 and 0.85. The same concrete composition is used as mentioned in 'Semi-adiabatic calorimetric measurements' section.

Thermal analysis

During thermogravimetric measurements the mass loss of a specimen heated up to 1123 K (850 °C) under an inert atmosphere is continuously measured. At temperatures lower than 378 K (105 °C), the evaporable water is driven off, whilst at higher temperatures the chemically bound water (w_b) dehydrates from the CH, C–S–H and other hydrates. However, to determine the value of the non-evaporable water content, the mass loss between 378 and

1123 K must be corrected for the mass loss due to decarbonation (around 923 K (650 °C)) [21].

The pastes were made with a *w*/*b* ratio of 0.5 and *s*/*b* ratios of 0, 0.30, 0.50 and 0.85. To avoid segregation and bleeding, the mixes were cast in cylindrical rotating moulds. After 1 day, the specimens were cured in a water bath. At the age of testing (ranging from 18 h to 3 years), the specimens were crushed and soaked in methanol for 1 week to stop the hydration. To limit the influence of the methanol treatment, the specimens were stored in a desiccator over silica gel for another week, as described by Baert [23].

BSE images

The hydration reaction of OPC and BFS can be visualized by BSE images. The five main phases, namely pores, C–S–H, CH, unhydrated BFS and unhydrated OPC can be distinguished from each other by their grey level. However, the grey level of BFS overlaps with these of unhydrated cement and CH. Because slag grains can be easily recognized by their typical angular shape, they are selected manually. The analysis of at least 15 images per sample allows representative calculations of the volume fractions of the phases at different times.

For this research, cement pastes with a *w*/*b* ratio of 0.5 and *s*/*b* ratios of 0, 0.50 and 0.85 were investigated at an age of 2 days and 28 months. The hydration was stopped by methanol replacement, as described above, and the specimens were subsequently placed in a desiccator, dried at 313 K (40 °C), impregnated with epoxy resin, and polished. Finally, the images were taken by an environmental SEM (ESEM).

Results and discussion

Isothermal calorimetry

Isothermal hydration curves

Figure 1 presents the change of the heat production rate *q* (mW/g binder) in time at 283, 293 and 308 K for the mixes in which an increasing percentage of OPC is replaced by BFS. As can be seen, higher curing temperatures accelerate the hydration of both binders, causing larger hydration peaks appearing earlier. Moreover, the presence of BFS influences the evolution of the heat production rate significantly. Besides the first (rapid reaction, not shown) and second hydration peak (hydration of C_3S), a third hydration peak can be distinguished for the mixes containing BFS. This peak corresponds to the slag reaction, initiated when the OPC hydration has liberated a sufficient amount of CH and the correct alkalinity is reached [10]. Secondly, BFS accelerates the OPC hydration as the second peak appears earlier with increasing BFS content (Fig. 1).

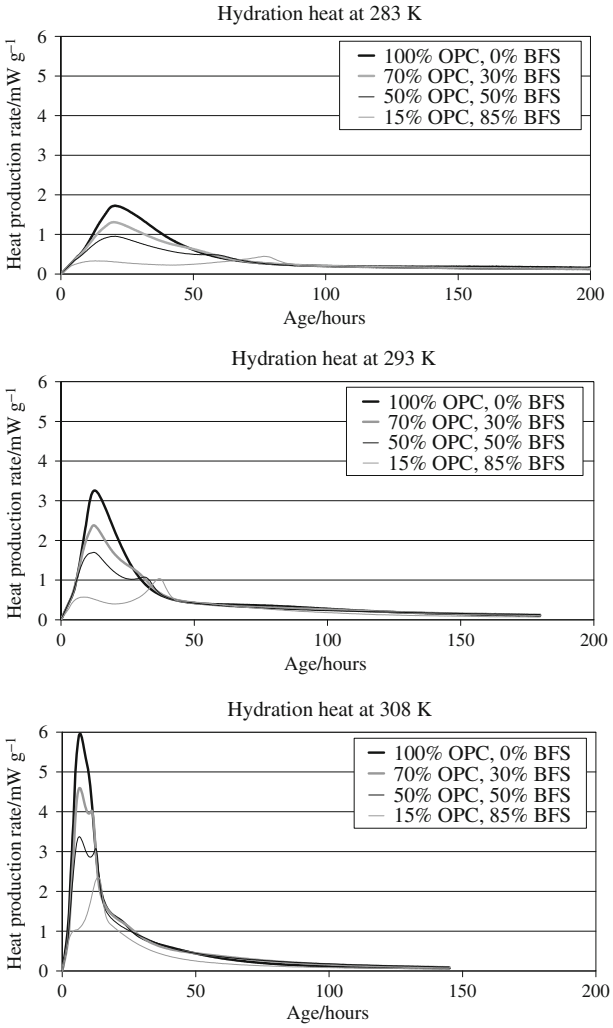

Fig. 1 Heat production rate q/mW g^{-1} in function of age under isothermal conditions (283, 293 and 308 K) for pastes with slag-to-binder ratios of 0, 30, 50 or 85%

Factors contributing towards the effect of BFS on the OPC hydration were summarized in the introduction and few of them are discussed below:

(1) Dilution effect: To investigate the importance of the dilution effect, isothermal calorimetric measurements were performed on cement pastes with water-to-cement ratios (*w*/*c*) equal to 0.5, 0.7, 1 and 3.3. These values correspond with *w*/*c* ratios in pastes for which *s*/*b* is, respectively, 0, 0.3, 0.5 and 0.85 and *w*/*b* is constant (= 0.5). The chemical composition of the cement and slag, used for these additional measurements, is mentioned in Table 1.
The experimental hydration curves, expressed in mW/g cement, can be found in Fig. 2. As can be seen, with

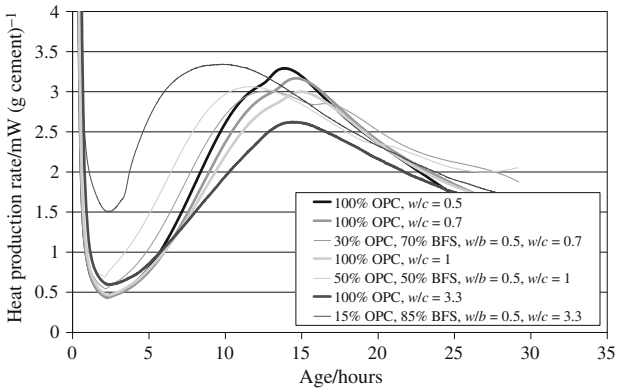

Fig. 2 Effect of the *w/c* ratio and addition of BFS on the hydration of OPC

increasing *w/c* ratio the second hydration peaks of the cement pastes decrease and appear slightly later. However, the pastes containing BFS show an acceleration of the C_3S hydration in comparison to their corresponding cement pastes with the same *w/c* and the reference paste. Moreover, the accelerating effect increases with increasing BFS content. In contrast to the measurements presented in Fig. 1, the maximum heat production rates for pastes containing slag are lower or equal to the maximum of the reference paste (in mW/g cement).

Based on these test results, the dilution effect (for *w/c* >0.5) has no acceleration effect and other factors are more important in the presence of slag.

(2) Heterogeneous nucleation: As mentioned above, BFS only possesses an accelerating influence when it has a very high specific surface. Nevertheless, a small accelerating effect on the C_3S (specific surface = 380 m^2/kg) hydration was noticed by Stark [19] in the presence of BFS (specific surface = 468 m^2/kg). In the research presented here, the fineness of the cement and slag is roughly equal (Table 1). Therefore, the contribution of heterogeneous nucleation is probably limited and other factors typical of slag will cause the acceleration of the cement hydration.

(3) Gypsum content: Based on the chemical composition of the cement and the slag (Table 1) and the formula of Bogue, the molar ratio nSO_3/nC_3A can be calculated for the pastes containing different amounts of BFS. Although slag has a lower SO_3 amount than clinker, the molar ratio increases with increasing BFS content when it is assumed that only OPC contains the mineral C_3A. The values of nSO_3/nC_3A are, respectively, 1.3, 1.6, 2.1 and 5.5 for pastes with *s/b* ratios of 0, 0.3, 0.5 and 0.85. Consequently, the conversion of ettringite to monosulfoaluminate decreases for pastes with increasing BFS content and the curve of the heat production rate in function of time changes. For molar ratios higher than 3, all C_3A is consumed by the first reaction of ettringite formation and higher values of the heat production rate are obtained at earlier ages [20].

Separation of the Portland cement reaction and slag reaction

In order to estimate the reaction degrees and activation energies of the cement and slag separately, a quite simple separation method is applied.

The separation of the OPC and BFS reaction was based on the cumulative heat production curve, as also proposed by Meinhard and Lackner [11] and presented in Fig. 3. For each paste, the part of the heat production originating from the slag reaction was calculated as the difference between the measured total heat production and the heat production of the reference mixture multiplied by the *c/b* ratio. Since this rescaled curve did not reach the values of the measured curve during the first hours when the slag hydration is still negligible and the OPC hydration was enhanced in presence of BFS ('Isothermal hydration curves' section), the scaling factors were increased in order to obtain a better fit (0.78, 0.58 and 0.22 instead of 0.70, 0.50 and 0.15). However, Figs. 1 and 3 show that the hydration curves of paste containing high amounts of slag (85%) differ from the others: the most dominant reaction is the slag hydration causing a larger heat production rate than the OPC reaction. Consequently, the second increase in the cumulative heat production curve is steeper than the initial increase.

As can be seen in Fig. 3, the time at which the slag hydration starts only depends on the environmental temperature and not on the cement replacement percentage. The higher the ambient temperature (283, 293 and 308 K), the earlier the slag reaction initiates (34, 22 and 9.5 h). Contrary to the model proposed by De Schutter [14], where the slag hydration lasts a few hours, an ongoing slag reaction, also at later ages, is assumed here. Neville [13] also recorded a continuing reaction of BFS over a long period.

Activation energy

The Arrhenius law given by Eq. 1 is a well-established function to describe the effect of the temperature θ (in K) on the reaction rate.

$$q_{\mathrm{P\ or\ S},\max,\theta} = q_{\mathrm{P\ or\ S},\max,293\mathrm{K}} \cdot \exp\left[\frac{E_{\mathrm{P\ or\ S}}}{R}\left(\frac{1}{293}-\frac{1}{\theta}\right)\right] \quad (1)$$

In this equation, E_P and E_S (kJ/mol) are the apparent activation energies for respectively the OPC and BFS

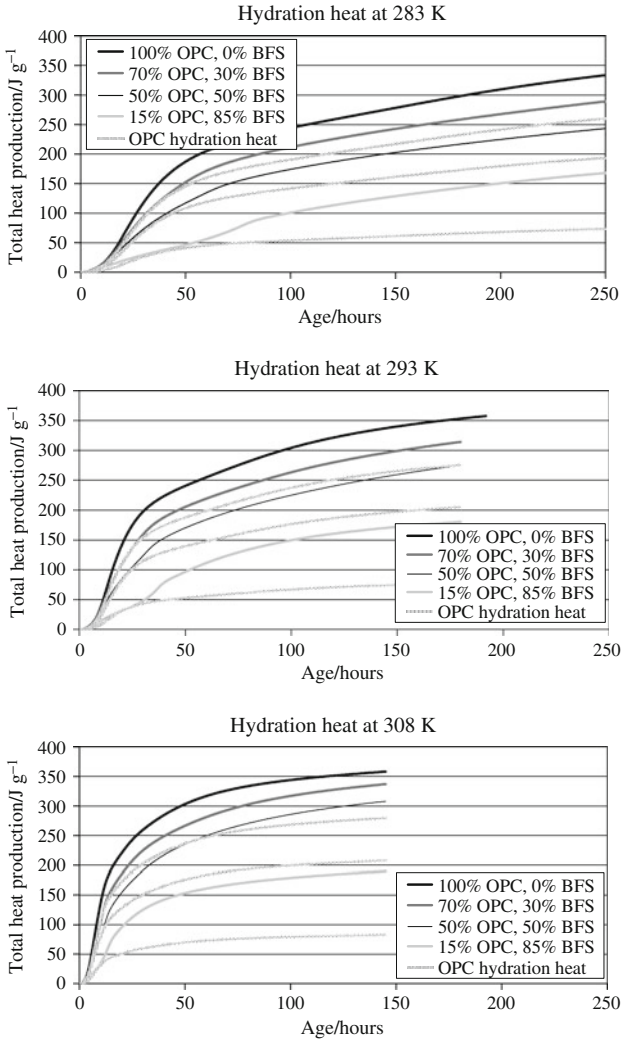

Fig. 3 Separation of the OPC and BFS reaction based on the cumulative heat production curves Q/J g^{-1} under isothermal conditions (283, 293 and 308 K) for pastes with slag-to-binder ratios of 0, 30, 50 or 85%

reaction and R is the universal gas constant with a value of 0.00831 kJ/mol/K. Since isothermal calorimetric measurements were performed at three different temperatures (283, 293 and 308 K), the apparent activation energies could be determined by non-linear regression analysis. A linear relationship was found between the c/b ratio and the activation energies as presented by Eqs. 2 and 3. Whilst E_P seems to increase with increasing BFS content, E_S seems to decrease.

$$E_P = -8.72 \cdot (c/b) + 39.416 \quad (2)$$

$$E_S = 26.38 \cdot (c/b) + 32.506 \quad (3)$$

In addition, a linear relationship was deduced between $q_{P,max,293K}$ and the c/b ratio given by Eq. 4 and between $q_{S,max,293K}$ and the s/b ratio given by Eq. 5.

$$q_{P,max,293K} = 11.965 \cdot (c/b) \quad (4)$$

$$q_{S,max,293K} = 3.880 \cdot (s/b) \quad (5)$$

The above-mentioned equations allow to predict values of E_P, E_S, $q_{P,max,293K}$ and $q_{S,max,293K}$ for pastes ($w/c = 0.5$) with other s/b ratios.

Semi-adiabatic calorimetry

The heat production rate q in function of time, determined under semi-adiabatic conditions, is presented in Fig. 4 for the different mixes. As with the isothermal calorimetric measurements, the first hydration peak is not shown. In comparison to Fig. 1, the heat production rate is higher, especially for the mixes with high cement contents. The temperature reached during hydration increases with decreasing BFS content and higher temperatures accelerate the cement hydration and slag reaction. For mortar samples with a cement-to-binder ratio (c/b) of 0.15 to 1, the maximum temperature ranges from 306 to 328 K (Table 2). The total heat (Q_{total}) liberated after 14 days, is summarized in Table 2. As can be seen, it decreases significantly for replacement percentages higher than 30%.

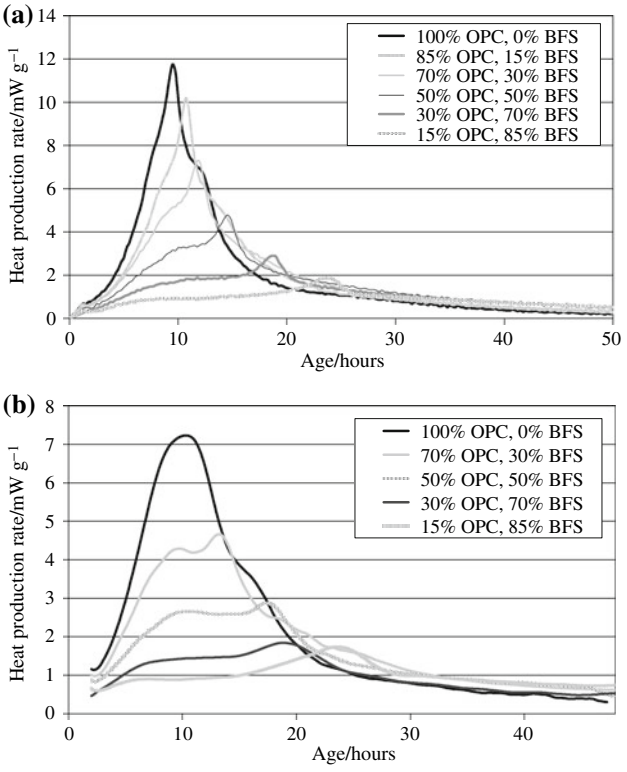

Fig. 4 Heat production rate q/mW g^{-1} in function of age under semi-adiabatic conditions for (**a**) mortars with slag-to-binder ratios of 0, 15, 30, 50, 70 or 85% and (**b**) concrete mixes with slag-to-binder ratios of 0, 30, 50, 70 or 85%

Table 2 Total hydration heat Q_{total}/J g^{-1} at 14 days and maximum temperature T_{max}/K under semi-adiabatic conditions (measured on mortar), compared to the total heat Q_∞ determined under isothermal conditions (293 K) by extrapolating the measured values on pastes to infinity, in function of slag-to-binder ratio (*s*/*b*)

s/*b*:	0	0.15	0.30	0.50	0.70	0.85
Q_{total}	411	411	400	363	308	253
T_{max}	328.0	325.5	321.0	315.0	309.5	306.0
Q_∞	433	–	406	395	–	243

Adiabatic calorimetry

In Fig. 5, the cumulative heat production and the heat production rate under adiabatic conditions of concrete containing different percentages of BFS is presented. However, limited heat losses are recorded with the adiabatic test setup, as can be seen in Fig. 5b. The cumulative heat production curves slightly decrease, indicating that the insulation is not perfect.

A comparison between the adiabatic and semi-adiabatic measurements on concrete is presented in Fig. 6. Since the temperature rise of a hydrating concrete sample is higher under adiabatic than semi-adiabatic conditions, the curves are presented in function of equivalent concrete age (at 293 K), calculated with the maturity function according to the Arrhenius law. The value of the activation energy was set to 33.5 kJ/mol [24]. The difference between the activation energy of BFS and OPC was not taken into account because of the difficulties in separating the slag and cement reaction. Moreover, the start of the cumulative heat production under semi-adiabatic conditions was corrected in correspondence with the adiabatic measurements, starting only 40 min after water addition. As can be seen, the correspondence between both methods seems to be good, considering the existing variation between experimental curves of the same mix.

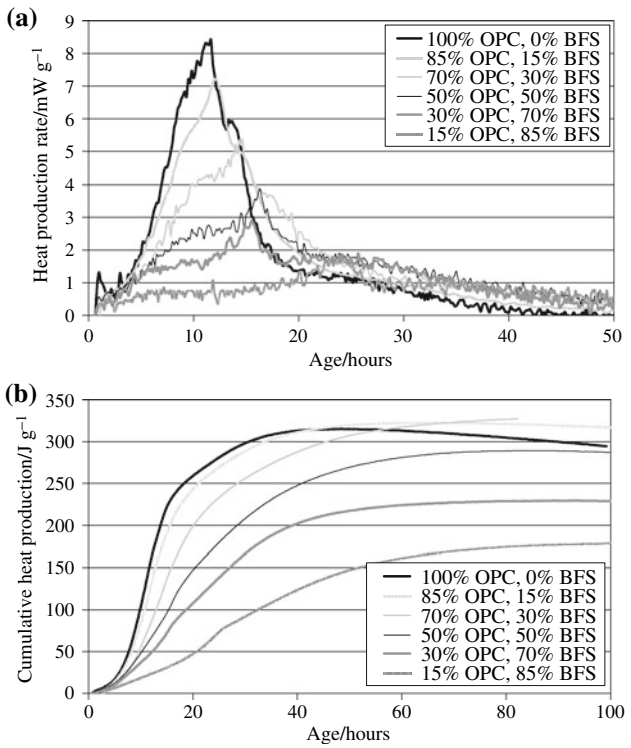

Fig. 5 Heat production rate/mW g^{-1} (**a**) and cumulative heat production/J g^{-1} (**b**) in function of concrete age under adiabatic conditions for concrete with slag-to-binder ratios of 0, 15, 30, 50, 70 or 85%

Thermogravimetry—chemically bound water

Figure 7 shows the non-evaporable water content (g/100 g binder) in function of time of pastes with a *s*/*b* ratio of 0, 0.30, 0.50 and 0.85. As can be seen, the bound water content of pastes containing BFS decreases less than proportional to the cement replacing percentage proving an enhancement of the cement hydration in presence of BFS at early ages and the considerable contribution of water bound to the slag hydration products at later ages.

The degree of reaction of OPC pastes can be obtained by normalizing w_b by its maximum value $w_{b,\infty}$. To determine $w_{b,\infty}$, the curve of w_b in function of time is fitted by a three parameter equation (Eq. 6), similar to the one proposed by [21]. τ and a, respectively, control the intercept and the curvature of the plot in the logarithmic scale. The resulting curves are presented in Fig. 7.

$$w_b = w_{b,\infty} \cdot \exp\left[-\left(\frac{\tau}{t}\right)^a\right] \quad (6)$$

For the cement paste, the estimated value of $w_{b,\infty}$ amounts to 23.8 g/100 g binder. This corresponds quite well with the values found in literature, ranging from 23 to 25% by mass of the anhydrous material for fully hydrated cement [13, 21, 25]. The same procedure was applied for the pastes containing 50 and 85% BFS. Whilst the value of $w_{b,\infty}$ for paste containing 50% BFS (22.4%) approximates the value of OPC paste, a sharp decline (11.4%) was recorded for paste in which 85% of the cement was replaced by BFS. According to Chen [26] the slag hydration degree and consequently the non-evaporable water content decreases significantly for high slag proportions.

Image analysis of BSE-images

The original and processed BSE-image at an age of 28 months of the cement paste in which 85% of the OPC was replaced by BFS is presented in Fig. 8, as an example. A summary of the average volume percentages cement, slag and water in the fresh mixtures and average volume

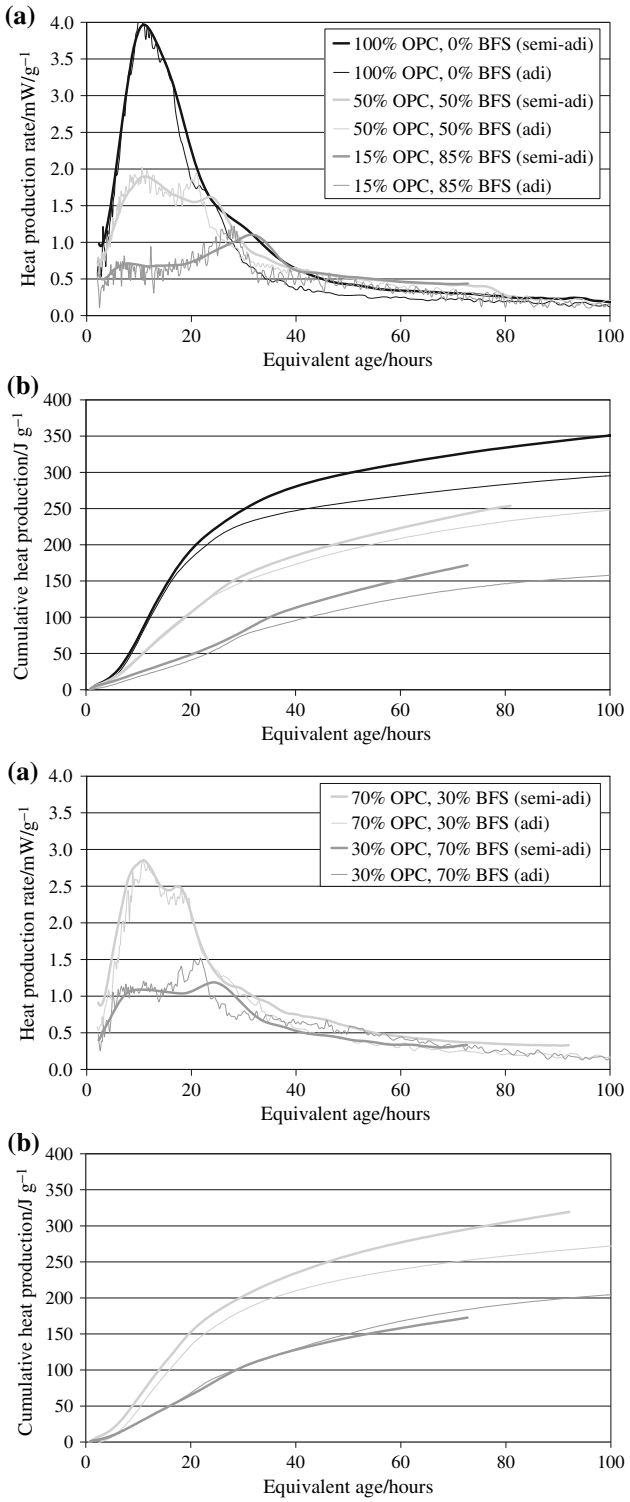

Fig. 6 Heat production rate/mW g^{-1} (**a**) and cumulative heat production/J g^{-1} (**b**) in function of equivalent age (at 293 K) of concrete containing 0–85% BFS under adiabatic and semi-adiabatic conditions

percentages pores, CSH, CH, unhydrated slag and unhydrated cement for each of the investigated hydrated samples is given in Table 3, respectively Table 4.

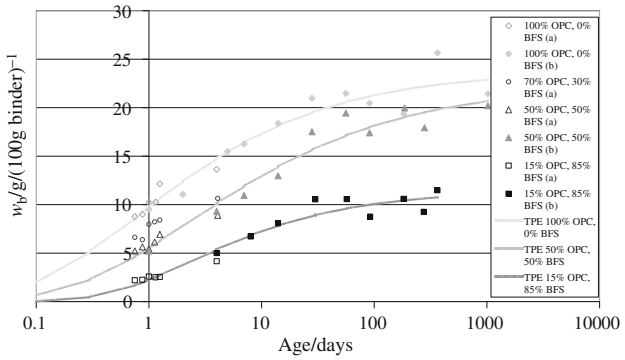

Fig. 7 Bound water content of cement paste containing 0, 30, 50 and 85% BFS in function of age

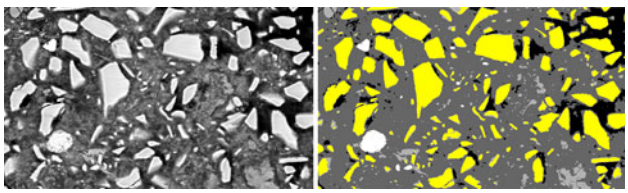

Fig. 8 BSE-image of a cement paste with slag-to-binder ratio = 0.85 at the age of 28 months (*left* original image, *right* same image with indication of the different phases: *black* pores, *dark grey* CSH, *light grey* CH, *yellow* unhydrated slag, *white* unhydrated cement)

Table 3 Volume fraction/% of cement, slag and pore water in the original samples (0 days) according to the slag-to-binder ratio (*s*/*b*)

s/*b*:	0	0.50	0.85
Cement	39.2	19.3	5.8
Slag	–	20.7	34.8
Pore water	60.8	60.0	59.4

Hydration degree versus reaction degree

The hydration degree can be determined based on BSE-images as the binder fraction which has reacted as shown by Eq. 7.

$$\alpha = \frac{\text{volume reacted binder}}{\text{initial volume binder}};$$

$$\alpha_P = \frac{\text{volume reacted OPC}}{\text{initial volume OPC}}; \alpha_S = \frac{\text{volume reacted BFS}}{\text{initial volume BFS}} \quad (7)$$

The experimental results are tabulated in Table 5. For OPC pastes, the hydration degree at 2 days amounts to 54% and increases up to 74% at 28 months. Since this value corresponds exactly with the ultimate hydration degree, calculated according to the formula of Mills [27] for $w/c = 0.5$ (Eq. 8), the hydration reaction is (almost) ended after 2 years. However, in the presence of slag, the ultimate hydration degree of cement seems to be more than 90%.

Table 4 Volume fraction/% of pores, unhydrated cement, unhydrated slag, C–S–H and CH in function of age and slag-to-binder (*s*/*b*) ratio, determined by BSE-images

	Early-age/2 days		Longer term/28 months		
s/*b*:	0	0.85	0	0.50	0.85
Unhydrated cement	17.8/s = 3.3	4.1/s = 2.6	10.2/s = 2.7	1.1/s = 0.4	0.5/s = 0.5
Unhydrated slag	–	33.5/s = 3.2	–	5.9/s = 1.9	21.2/s = 3.2
Pore	29.5/s = 6.8	38.4/s = 3.4	12.3/s = 3.9	13.6/s = 3.9	19.2/s = 7.9
C–S–H	43.7/s = 7.5	22.5/s = 2.0	64.9/s = 2.3	72.6/s = 2.7	55.8/s = 6.4
CH	8.8/s = 3.1	1.5/s = 1.8	12.6/s = 3.2	6.9/s = 1.9	3.3/s = 1.8

This confirms the enhanced cement hydration in the presence of BFS for which the contributing factors are summarized in the introduction.

$$\alpha_u = \frac{1.031 \cdot w/c}{0.194 + w/c} \tag{8}$$

The hydration degree of slag in paste is difficult to predict and depends on the curing conditions, test ages, *w*/*b*, *c*/*s* and the slag reactivity. Chen [26] proposed a tentative degree of 70% for slag in blended cement paste. From experiments in this research, a hydration degree of 72% for pastes containing 50% slag was found. However, when 85% of the cement was replaced by BFS, the hydration degree of slag decreased to 39%. This agrees with the findings of Chen [26], stating that the effect of *s*/*c* on the slag reactivity is limited for low slag proportions and that the reactivity decreases significantly for *s*/*b* >0.80.

On the other hand, the reaction degree is introduced as an approximation of the hydration degree. Considering the ultimate hydration degree of the pastes, both parameters can be compared. In this research, the reaction degree was calculated in two different ways. Firstly, for the isothermal calorimetric measurements (293 K), the reaction degree was defined by Eq. 9 as the ratio of the heat liberated at a certain moment $Q(t)$ to the total heat Q_∞. In accordance with 'Thermogravimetry—chemically bound water' section, the total heat at infinity was here determined by Eq. 6 with *w* replaced by *Q*. A comparison between the total heat determined according to this calculation method (Q_∞) and the values obtained after 14 days hydration under semi-adiabatic conditions (Q_{total}) ('Semi-adiabatic calorimetry' section) can be found in Table 2. The results of both methods coincide quite well, although the last-mentioned method gives generally slightly lower values, probably due to the measuring method and time.

$$r_Q(t) = \frac{Q(t)}{Q_\infty} \tag{9}$$

Secondly, TG allowed to determine the overall reaction degree as the ratio of the bound water content at a certain moment to the maximum content (Eq. 10).

$$r_w(t) = \frac{w_b(t)}{w_{b,\infty}} \tag{10}$$

Both calculation methods of the overall reaction degree, for ages ranging from 18 h till 7 days, were compared and presented in Fig. 9. As can be seen, the parameters coincide for ages younger than 2 days. At later ages, the reaction degree determined by isothermal calorimetry yields slightly higher values than the reaction degree determined by thermogravimetric measurements.

Finally, for mixes with replacement percentages less than 70%, 'Separation of the Portland cement reaction and slag reaction' section explains the separation of the total heat in two parts, one due to the OPC hydration and the other due to the BFS reaction. This allows to define distinct reaction degrees for the cement and slag hydration

Table 5 Hydration degree/%, determined by image analysis of BSE-images

	Early-age/2 days		Longer term/28 months		
s/*b*:	0	0.85	0	0.50	0.85
α	54	7	74	83	47
α_P	54	29	74	94	91
α_S	–	4	–	72	39

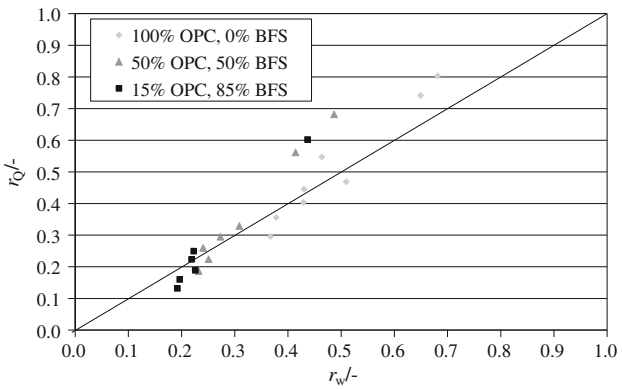

Fig. 9 Comparison between the reaction degree determined by isothermal calorimetry ($r_Q = Q/Q_\infty$) and TG ($r_w = w_b/w_{b\infty}$)

Table 6 Reaction degree/%, determined by isothermal (293 K) calorimetric measurements

	Early-age/2 days		Longer term/7 days		
s/*b*:	0	0.85	0	0.50	0.85
r	57	37	87	75	71
r_P	57	/	87	87	/
r_S	–	/	–	54	/

The separation of both reactions is defined based on the description in 'Separation of the Portland cement reaction and slag reaction' section. Values not corrected for the ultimate hydration degree

'/' means that these values could not be calculated; '–' means that these values do not exist

(Eq. 11). The results at 2 and 7 days are tabulated in Table 6.

$$r = \frac{Q}{Q_{\text{total}}}; \quad r_P = \frac{Q_{\text{OPC}}}{Q_{\text{OPC,total}}}; \quad r_S = \frac{Q_{\text{BFS}}}{Q_{\text{BFS,total}}} \tag{11}$$

At 2 days, the reaction degree of OPC, amounted to 57%. Considering the ultimate hydration degree ($\sim$74%), this value seems to be low in comparison with the measured hydration degree at that time ($\sim$54%). On the contrary, for pastes containing 85% of the cement replaced by slag, the reaction degree (37%) is higher in comparison to the results of the BSE-images.

At 7 days, the overall reaction degrees increased significantly and amounted to 87% for pure cement paste and 75% for paste containing 50% slag. For the last-mentioned mix, the values of r_P and r_s are, respectively, 87 and 54%, indicating that most of the cement particles are hydrated at that time, whilst half of the slag particles are still unhydrated.

Conclusions

The hydration process of paste containing OPC blended with BFS (s/b = 0, 0.30, 0.50, 0.85) and a w/b ratio = 0.5 was investigated by thermogravimetry and isothermal calorimetry at early age. For pastes with slag, an additional hydration peak due to the BFS reaction was recorded and an acceleration of the OPC hydration in presence of BFS was noticed. Moreover, both methods allowed to determine the overall reaction degree, respectively, by the ratio $w_b(t)/w_{b\infty}$ (w_b = bound water content) or $Q(t)/Q_\infty$ (Q = cumulative heat production). At early ages, both calculations corresponded well. The values at infinity ($w_{b\infty}$ and Q_∞) were estimated by extrapolating the data, using a non-linear regression curve. Whilst the value of $w_{b,\infty}$ was about the same for OPC paste and paste containing 50% BFS, a sharp decline was recorded for pastes in which 85% of the cement was replaced by BFS. Furthermore, only a slight difference was noticed between Q_∞ and the total heat released after 14 days under semi-adiabatic conditions.

In addition, the hydration was visualized by BSE-images at 2 days and 28 months. Based on these images, the hydration degree was determined. After 28 months, the hydration degree of cement paste amounted to 74%, which corresponds with the ultimate hydration degree predicted by Mills [27]. For the pastes containing BFS, the hydration degree of OPC increased above 90%. The hydration degree of BFS is about 70%, except for high replacement percentages. In this case, the slag reactivity decreases significantly and a hydration degree of 39% is reached for pastes with s/b = 0.85.

Acknowledgements As Research Assistants of the Research Foundation—Flanders (FWO-Vlaanderen), the authors Elke Gruyaert and Nicolas Robeyst want to thank the foundation for the financial support. Moreover, this study was supported in part by grant no. BOF/B/05928/01 from the Universtiy of Ghent (BOF—Bijzonder Onderzoeksfonds).

References

1. Mostafa NY, Brown PW. Heat of hydration of high reactive pozzolans in blended cements: isothermal conduction calorimetry. Thermochim Acta. 2005;435:162–7.
2. Shi C, Dau RL. Some factors affecting early hydration of alkali-slag cements. Cem Concr Res. 1999;26:439–47.
3. Zhou J, Ye G, Van Breugel K. Hydration of Portland cement blended with blast furnace slag at early age. In: Marchand J, Bissonnette B, Gagné R, Jolin M, Paradis F, editors. Second International Symposium on Advances in Concrete through Science and Engineering. Québec; 2006.
4. Wadsö L. Using isothermal (heat conduction) calorimetry to study the effect of mixing intensity on reaction rate of cement mortars. In: Beadoin JJ, Makar JM, Raki L, editors. 12th International Congress on the Chemistry of Cement. Montréal; 2007.
5. Evju C. Initial hydration of cementitious systems using a simple isothermal calorimeter and dynamic correction. J Therm Anal Calorim. 2003;71:829–40.
6. Schindler AK, Folliard KJ. Influence of supplementary cementing materials on the heat of hydration of concrete. In: Ninth Conference on Advances in Cement and Concrete. Colorado; 2003.
7. Bensted J. Some application of conduction calorimetry to cement hydration. Adv Cem Res. 1987;1:35–44.
8. Baert G. Physico-chemical interactions in Portland cement-(high volume) fly ash binders. Ghent: Ghent University. PhD; 2009.
9. Taylor H. Cement chemistry. 2nd ed. London: Thomas Telford Publishing; 1997.
10. Hewlett PC. Lea's chemistry of cement and concrete. London: Elsevier; 1998.
11. Meinhard K, Lackner R. Multi-phase hydration model for prediction of hydration-heat release of blended cements. Cem Concr Res. 2008;38:794–802.
12. Song S, Sohn D, Jennings HM, Mason TO. Hydration of alkali-activated ground granulated blast-furnace slag. J Mater Sci. 2000;35:249–57.
13. Neville AM. Properties of concrete. Essex: Longmen; 1995.
14. De Schutter G, Taerwe L. General hydration model for Portland cement and blast furnace slag cement. Cem Concr Res. 1995;25:593–604.

15. Bougara A, Lynsdale C, Milestone NB. Reactivity and performance of blast-furnace slags of different origin. Cem Concr Compos. 2010;32:319–24.
16. Escalante-Garcia JI, Sharp JH. The chemical composition and microstructure of hydration products in blended cements. Cem Concr Compos. 2004;26:967–76.
17. Singh NB, Bhattacharjee KN, Shukla AK. Hydration of Portland blended cements. Cem Concr Res. 1995;25:1023–30.
18. Escalante-Garcia JI, Sharp JH. Effect of temperature on the hydration of the main clinker phases in Portland cements: Part II, blended cements. Cem Concr Res. 1998;28:1259–74.
19. Stark J, Möser B, Bellmann F. Nucleation and growth of C–S–H phases on mineral admixtures. In: Grosse CU, editor. Advances in construction materials. Berlin: Springer; 2007. p. 231–538.
20. D'Aloia L, Chanvillard G. Determining the "apparent" activation energy of concrete: Ea-numerical simulations of the heat of hydration of cement. Cem Concr Res. 2002;32:1277–89.
21. Pane I, Hansen W. Investigation of blended cement hydration by isothermal calorimetry and thermal analysis. Cem Concr Res. 2005;35:1155–64.
22. De Schutter G. Hydration and temperature development of concrete made with blast-furnace slag cement. Cem Concr Res. 1999;29:143–9.
23. Baert G, Hoste S, De Schutter G, De Belie N. Reactivity of fly ash in cement paste studied by means of thermogravimetry and isothermal calorimetry. J Therm Anal Calorim. 2008;94:485–92.
24. Robeyst N. Monitoring setting and microstructure development in fresh concrete with the ultrasonic through-transmission method. Ghent: Ghent University. PhD; 2009.
25. Copeland LE, Kantro DL. Chemistry of hydration of Portland cement. In: Symposium on the Chemistry of Cement. Washington: Cement and Concrete Association; 1960. p. 429.
26. Chen W. Hydration of slag cement—theory, modeling and application. Enschede: University of Twente. PhD; 2006.
27. Mills RH. Factors influencing cessation of hydration in water-cured cement pastes. In: Board HR, editor. Symposium on the Structure of Portland Cement Paste and Concrete. Washington, D.C.; 1966. p. 406.